

# SPARSE PRECISION MATRIX SELECTION FOR FITTING GAUSSIAN RANDOM FIELD MODELS TO LARGE DATA SETS

S. DAVANLOO TAJBAKSH†, N. S. AYBAT†, AND E. DEL CASTILLO†

**Abstract.** Fitting a Gaussian Random Field (GRF) model to spatial data via maximum likelihood (ML) requires optimizing a highly non-convex function. Iterative methods to solve the ML problem require  $O(n^3)$  floating point operations per iteration, where  $n$  denotes the number of data points. For large data sets, the non-convexity and computational complexity of the ML problem render covariance ML methods inefficient for GRF fitting. In this paper, we propose a new two-step GRF estimation procedure when the process is stationary with an isotropic covariance function. First, a *convex* likelihood problem, regularized with a weighted  $\ell_1$ -norm based on available inter-point distance information, is solved to fit a sparse *precision* (inverse covariance) matrix to the GRF model using the Alternating Direction Method of Multipliers. Second, the parameters of the GRF spatial covariance function are estimated using a simple line search. Numerical experiments show improvements of one order of magnitude in mean square prediction error over competitor methods. The covariance parameters estimated by the proposed approach are shown to be more precise and accurate than those obtained with alternative methods. Large datasets are handled by a blocking scheme that enables parallel computation and ensures without further formulation that the predicted surface has no discontinuities at the block boundaries. The proposed approach can be easily modified to allow fitting non-stationary GRF processes.

**Key words.** Convex Optimization, Gaussian Markov Random Fields, Covariance Selection, Spatial Statistics, ADMM.

**1. Introduction.** Gaussian Random Field (GRF) models<sup>1</sup> are widely used in several fields including Machine Learning, Geostatistics, Computer Experiments (metamodeling) and industrial metrology. Traditional methods for fitting a GRF model from sample data rely on maximum likelihood estimation (MLE) of the parameters of an assumed spatial covariance matrix. As it is well-known in the Spatial Statistics area [43], the log-likelihood function for the covariance parameters of a GRF is highly non-concave, which leads to numerical difficulties if standard optimizers are applied for MLE, yielding suboptimal estimates that do not share the nice properties of MLEs. Furthermore, MLE requires  $O(n^3)$  operations per iteration of the optimization routine (where  $n$  is the number of data points) given the necessary covariance matrix inversions, which renders the method inefficient for large data sets. This is what [2] called the “Big  $n$  problem” in GRF modeling.

To overcome these difficulties, in this paper we present a new method for fitting a GRF from a single observed realization of the process. Our proposed Sparse Precision matrix Selection (SPS) method first estimates a sparse precision (inverse covariance) matrix corresponding to the GRF, by solving a *convex* regularized likelihood problem that uses the available inter-point distance information in a weighted  $\ell_1$  regularization term. This precision matrix is not parameterized in any form and constitutes a Gaussian Markov Random Field (GMRF) approximation to the GRF. This first stage problem is solved with a variant of the Alternating Direction Method of Multipliers (ADMM) algorithm, which has linear convergence rate. In the second stage, covariance matrix parameters are estimated solving a least squares problem which provides more consistent estimates than those obtained by solving the MLE problem, and the second stage problem can be solved with a line search in the range parameter for stationary isotropic GRFs. Empirical evidence suggests that the first stage optimization “zooms-in” to a region in the covariance parameter space that is close to true covariance parameters; hence, the fitted parameters and the resulting prediction estimates are much more competitive than the maximum likelihood estimates obtained with other methods. We next provide some preliminaries, including a brief review of other methods to which our SPS approach will be compared to.

**1.1. Preliminaries.** Let  $\mathcal{X} \subseteq \mathbb{R}^d$ , and the observed dataset be a realization of a latent GRF  $f : \mathcal{X} \rightarrow \mathbb{R}$  with additive Gaussian noise:

$$y(\mathbf{x}) = f(\mathbf{x}) + \epsilon, \quad (1.1)$$

where  $f(\mathbf{x})$  has a mean function  $m_f(\mathbf{x})$  and a covariance function  $c_f(\mathbf{x}, \mathbf{x}') = \text{cov}(f(\mathbf{x}), f(\mathbf{x}'))$ , and  $\epsilon \sim N(0, \theta_0^*)$  is independent of  $f(\mathbf{x})$  for all  $\mathbf{x} \in \mathcal{X}$ . We assume that the training data set  $\mathcal{D} = \{(\mathbf{x}_i, y_i)\}_{i=1}^n$

<sup>†</sup>Department of Industrial and Manufacturing Engineering, The Pennsylvania State University, University Park, PA 16802. Emails: sdt144@psu.edu, nsa10@psu.edu, exd13@psu.edu.

<sup>1</sup>A GRF is also called a Gaussian Process (GP) model or simply a Gaussian Field (GF).

contains  $n$  observations  $y_i$  at  $n$  distinct locations  $\mathbf{x}_i \in \mathcal{X}$ ; hence, there is *one replicate* per location. Let  $\mathbf{y} \in \mathbb{R}^n$  denote the vector of observations in  $\mathcal{D}$ . Given a new location  $\mathbf{x}_0 \in \mathcal{X}$ , a usual goal in GRF modeling is to predict  $f_0 := f(\mathbf{x}_0)$ . Without loss of generality, we further assume that the GRF has a constant mean equal to zero, i.e.  $m_f(\mathbf{x}) = 0$ . Since any countable collection of observations from a GRF follows a multivariate normal distribution, the joint distribution of  $(\mathbf{y}^T, f_0)^T$  is given by

$$\begin{pmatrix} \mathbf{y} \\ f_0 \end{pmatrix} \sim N_{n+1} \left( \mathbf{0}_{n+1}, \begin{bmatrix} C_f + \theta_0^* \mathbf{I}_n & \mathbf{c}_0 \\ \mathbf{c}_0^T & c_{00} \end{bmatrix} \right), \quad (1.2)$$

where  $c_{00} = c_f(\mathbf{x}_0, \mathbf{x}_0)$ ,  $\mathbf{c}_0^T = [c_f(\mathbf{x}_1, \mathbf{x}_0), \dots, c_f(\mathbf{x}_n, \mathbf{x}_0)]$ , and the covariance matrix  $C_f \in \mathbb{R}^{n \times n}$  is formed such that its  $(i, j)^{th}$  element is equal to  $c_f(\mathbf{x}_i, \mathbf{x}_j)$ . Therefore, the conditional distribution of  $f_0$  given  $\mathbf{y}$  (i.e., the *predictive distribution* of  $f_0$ ), is given as

$$p(f_0 | \mathbf{y}) = N(\mathbf{c}_0^T (C_f + \theta_0^* \mathbf{I}_n)^{-1} \mathbf{y}, c_{00} - \mathbf{c}_0^T (C_f + \theta_0^* \mathbf{I}_n)^{-1} \mathbf{c}_0). \quad (1.3)$$

The mean of this predictive distribution is a point estimate (known as the *Kriging* estimate in Geostatistics) and its variance measures the uncertainty of this prediction.

It is clear from the form of the predictive distribution that the prediction performance heavily relies on the correct estimation of the unknown covariance function. This estimation is simplified by assuming that the unknown covariance function  $c_f$  belongs to a parametric family of covariance functions,  $\{c_f(\boldsymbol{\theta}_f, \mathbf{x}, \mathbf{x}') : \boldsymbol{\theta}_f \in \Theta_f\}$ , where  $\Theta_f$  is a set that contains the true parameters  $\boldsymbol{\theta}_f^*$  of the  $f$ -process. This is a common practice that originates in the Geostatistics literature (see, e.g., [8]). The main property of any covariance function is that it should lead to a positive definite covariance matrix for any finite set of fixed locations  $\{\mathbf{x}_i\}_{i=1}^n \subset \mathcal{X}$ . Let  $\boldsymbol{\theta}^* = [\theta_0^*, \boldsymbol{\theta}_f^{*T}]^T \in \Theta$  denote the unknown true parameters of the  $y$ -process, where  $\Theta := \mathbb{R}_+ \times \Theta_f$ . Hence,  $c(\boldsymbol{\theta}^*, \mathbf{x}, \mathbf{x}') := c_f(\boldsymbol{\theta}_f^*, \mathbf{x}, \mathbf{x}') + \theta_0^* \delta(\mathbf{x}, \mathbf{x}')$  denote the covariance function of the  $y$ -process. Here  $\delta(\cdot, \cdot)$  denotes the indicator function, i.e.  $\delta(\mathbf{x}, \mathbf{x}') = 1$  if  $\mathbf{x} = \mathbf{x}'$ , and equal to 0 otherwise.

Given a set of locations  $\{\mathbf{x}_i\}_{i=1}^n$ , and  $\boldsymbol{\theta} = [\theta_0, \boldsymbol{\theta}_f^T]^T \in \Theta$ , let  $C_f(\boldsymbol{\theta}_f) \in \mathbb{R}^{n \times n}$  be such that its  $(i, j)^{th}$  element is equal to  $c_f(\boldsymbol{\theta}_f, \mathbf{x}_i, \mathbf{x}_j)$ , and define  $C(\boldsymbol{\theta}) := C_f(\boldsymbol{\theta}_f) + \theta_0 \mathbf{I}_n$ , i.e. its  $(i, j)^{th}$  element is equal to  $c(\boldsymbol{\theta}, \mathbf{x}_i, \mathbf{x}_j)$ . Hence,  $C_f(\boldsymbol{\theta}_f^*)$  and  $C(\boldsymbol{\theta}^*)$  denote the true covariance matrices of the  $f$ -process and  $y$ -process, respectively, corresponding to locations  $\{\mathbf{x}_i\}_{i=1}^n$ . The log marginal likelihood function  $\ell(\boldsymbol{\theta}) := \log p(\mathbf{y} | \boldsymbol{\theta}, \{\mathbf{x}_i\}_{i=1}^n)$  can be written as

$$\ell(\boldsymbol{\theta}) = -\frac{1}{2} \log \det(C(\boldsymbol{\theta})) - \frac{1}{2} \mathbf{y}^T (C(\boldsymbol{\theta}))^{-1} \mathbf{y} - \frac{n}{2} \log(2\pi). \quad (1.4)$$

Hence, finding the MLE of the  $y$ -process parameters requires solving the following optimization problem:

$$\hat{\boldsymbol{\theta}}_{MLE} = \underset{\boldsymbol{\theta} \in \Theta}{\operatorname{argmin}} \log \det(C(\boldsymbol{\theta})) + \mathbf{y}^T (C(\boldsymbol{\theta}))^{-1} \mathbf{y}. \quad (1.5)$$

Note that the set  $\Theta = \mathbb{R}_+ \times \Theta_f$  contains the true unknown parameters  $\boldsymbol{\theta}^* = [\theta_0^*, \boldsymbol{\theta}_f^{*T}]^T$ .

The log-likelihood function  $\ell(\boldsymbol{\theta})$  is *not* concave for many important parametric families of covariance functions, e.g. Matern or Powered-Exponential. Therefore, the MLE problem in (1.5) is *non-convex*, which makes the likelihood-based parameter estimation a very difficult problem since it causes standard optimization routines to be trapped in local minima ([?, 30], [4] p. 311).

Empirical evidence from our numerical experiments reported below suggests the reason why the 2-stage SPS approach works significantly better compared to other well-known one-step *non-convex* log-likelihood maximization approaches. Basically, deferring to deal with non-convexity to a later stage and obtaining a regularized log-likelihood estimation of the precision matrix through solving a convex problem first, we obtain a second stage non-convex least-squares problem of which global minimum is “very close” to the true model parameters; moreover, there are no other local extrema in a considerably “large” neighborhood of the global minimum- see Figure 3.1.

Furthermore, our SPS algorithm can be utilized for fitting a GRF to large data sets by partitioning the input space  $\mathcal{X}$  into smaller regions or blocks such that for each region, it is feasible to estimate the corresponding precision matrix with the available computational resources. Note that it is possible to parallelize this estimation process if multiple processing units are available.

Several other methods have been proposed in the literature to deal with the “Big  $n$ ” problem in GRF modeling. These approaches can be broadly classified in six main classes: 1) *Likelihood approximation methods* approximate the likelihood function in the spectral domain [15, 40], or approximate it as a product of conditional densities [42, 41]; 2) *Covariance tapering* provides a sparse covariance matrix in which the long range (usually weak) covariance elements are set to zero. Sparse matrix routines are then used to efficiently find the inverse and determinant of the resulting matrix [17]; 3) *Low-rank process approximation methods* are based on a truncated basis function expansion of the underlying GRF which results in reducing the computational complexity from  $O(n^3)$  to  $O(r^3)$ , where  $r$  is the number of basis functions used to approximate the process [22, 7, 2, 33]; 4) *Sampling-based stochastic approximation* draws a small number  $m$  of sample data points ( $m \ll n$ ) at each iteration and the model parameters are updated according to a stochastic approximation technique until the convergence is achieved [27]; 5) *Localized GRFs* splits the input domain into different segments, and the covariance parameters are estimated via ML locally on each segment [19]. This type of approach requires further formulation to avoid discontinuities in the predicted surface over the full domain [34]; and finally 6) *Markov random field approximations*, related to our proposed SPS method, that will be discussed in more detail in Section 2. In addition, there are some methods that fall in the intersection of two classes: [37] have combined low-rank process approximation with covariance tapering; the approach proposed by [39] is a mix of likelihood approximation and localized GRF.

The rest of the present paper is organized as follows: in Section 2, we motivate the proposed method. In Section 3 we discuss the two-stage SPS algorithm and its extension to big dataset applications. It is shown that the first stage of our method has linear convergence, while the second stage can be solved efficiently via a line search for isotropic GRFs. Next, in Section 4, we evaluate numerically the prediction performance of the proposed method comparing it to alternative methods in the literature using both synthetic and real data. Finally, Section 5 concludes by providing some summarizing remarks and directions for further research.

**2. Motivation for the proposed SPS method.** The proposed method can be motivated by providing four interrelated remarks: *a)* the precision matrix  $P^* \in \mathbb{R}^{n \times n}$  of a stationary isotropic GRF corresponding to a given set of  $n$  locations  $\{\mathbf{x}_i\}_{i=1}^n$  can usually be approximated with a sparse matrix; *b)* powerful convex optimization algorithms exist to solve Sparse Covariance Selection problems which can be used to find a sparse precision matrix; *c)* the past and recent work on directly approximating a GRF with a GMRF also involves determining a sparse precision matrix; *d)* the available distance information can be incorporated into the GRF estimation algorithm. In this section we discuss each of these motivations.

*a)* Let  $\boldsymbol{\theta}^* \in \Theta$  denote the true parameters, and  $C^* = C(\boldsymbol{\theta}^*)$  denote the true covariance matrix of the  $y$ -process corresponding to given set of locations  $\{\mathbf{x}_i\}_{i=1}^n$ . Note that the sparsity patterns of  $C(\boldsymbol{\theta}^*)^{-1} = (C_f(\boldsymbol{\theta}_f^*) + \theta_0^* \mathbf{I}_n)^{-1}$  and  $C(\boldsymbol{\theta}_f^*)^{-1}$  are the same for all  $\theta_0^* \geq 0$ . Hence, without loss of generality, we assume that  $\theta_0^* = 0$  for the simplicity of the following discussion. Our proposed method is partially based on the empirical observation that the precision matrix  $P^* = C(\boldsymbol{\theta}^*)^{-1}$  of a stationary isotropic GRF can be approximated by a sparse matrix. The element  $P_{ij}^*$  of the precision matrix is a function of the conditional covariance (also known as *partial covariance*) between the variables  $y(\mathbf{x}_i)$  and  $y(\mathbf{x}_j)$  given all the remaining ones:

$$P_{ij}^* = \frac{-\text{Cov}(y(\mathbf{x}_i), y(\mathbf{x}_j) \mid \{y(\mathbf{x}_k)\}_{k \neq i,j})}{\text{Var}(y(\mathbf{x}_i) \mid \{y(\mathbf{x}_k)\}_{k \neq i,j}) \text{Var}(y(\mathbf{x}_j) \mid \{y(\mathbf{x}_k)\}_{k \neq i,j}) - \text{Cov}(y(\mathbf{x}_i), y(\mathbf{x}_j) \mid \{y(\mathbf{x}_k)\}_{k \neq i,j})^2}.$$

It is clear from the above identity that  $|P_{ij}^*| \rightarrow 0$  as  $\text{Cov}(y(\mathbf{x}_i), y(\mathbf{x}_j) \mid \{y(\mathbf{x}_k)\}_{k \neq i,j}) \rightarrow 0$ . In particular, *conditionally independent* variables lead to a zero entry in the precision matrix [44]. This is the reason why sparse precision matrices are common in graphical models and Bayesian networks [32, 44] where most pairs of variables are independent when conditioned on the remaining ones.

That the precision matrix of a GRF is close to sparse is related to the interesting behavior of the so-called *screen effect* in a spatial process ([8], p. 133, [24], p. 346). The screen effect is complete in  $\mathbb{R}^1$ , i.e. for given three data points on a line, the two outer points are conditionally independent (in time series models, the partial (auto)correlation function “cuts off” after lag  $k$  for a Markovian  $\text{AR}(k)$  process –see [5]). However, for a GRF in  $\mathbb{R}^d$  with  $d > 1$  the screen effect is *not* complete and hence the corresponding precision matrix is not sparse for any *finite* set of variables pertaining to the GRF. However, for all covariance functions tested (for stationary GRFs), we have empirically observed that for a finite set of locations the magnitude of the off-diagonal elements of the *precision* matrix decays exponentially to 0 when these elements are sorted in

decreasing order, with a decay that is much faster than that observed in the elements of the covariance matrix. To illustrate this fact, we compared the decay in covariance and precision matrix elements in Figure 2.1 for data generated from GRFs with Matern- $\frac{3}{2}$ , Squared Exponential, and Exponential covariance functions – for the functional form of these covariance functions, see Appendix A. Hence, the precision matrix can be better approximated by a sparse matrix than the covariance matrix can be, i.e. the number of elements of the precision matrix that are greater than a given threshold in magnitude is significantly smaller than the corresponding number of elements of the covariance matrix.

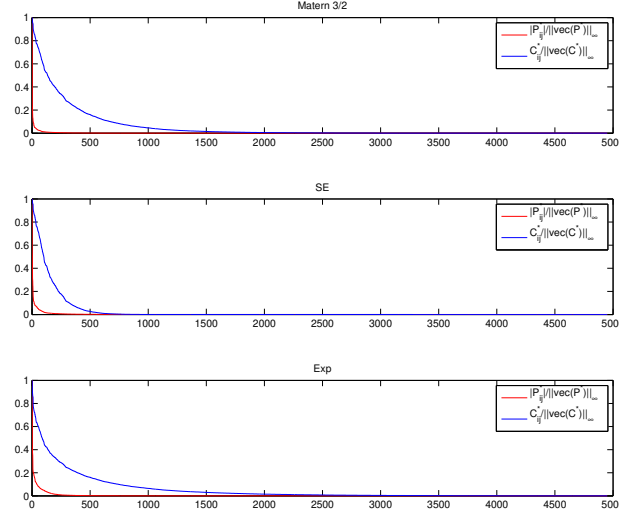


Fig. 2.1: Illustration of the near-sparse behavior of the Precision and Covariance matrices of a GRF. Graphs show the absolute values of the unique off-diagonal elements of the precision and covariance matrices ( $P_{ij}^*$  and  $C_{ij}^*$ , scaled by their maximums) sorted in descending order plotted versus their rank. The underlying GRF was evaluated over a set of 100 randomly selected points in  $\mathcal{X} = \{\mathbf{x} \in \mathbb{R}^2 : -50 \leq \mathbf{x} \leq 50\}$  for three different covariance functions with range parameter equal to 10 and variance parameter equal to 1.

By fixing the domain of the process and increasing  $n$  (increasing the density of the data points), the screen effect becomes much stronger, i.e. off-diagonal entries decay to 0 much faster. Hence, the precision matrices become closer to a sparse matrix as  $n$  increases in a fixed domain. To illustrate this phenomenon numerically, we calculate the precision matrices corresponding to data generated from a Matern GRF with parameters  $\nu = 3/2$ , variance equal to 1, and range equal to 10 for  $n \in \{10, 100, 1000\}$  over a *fixed* squared domain of size 100, i.e.  $\mathcal{X} = \{\mathbf{x} \in \mathbb{R}^2 : -50 \leq \mathbf{x} \leq 50\}$ . Then, as a measure of near-sparsity, we computed the percentage of scaled off-diagonal elements in the precision matrix greater in absolute value than certain threshold values ( $\epsilon = 0.1, 0.01, 0.001$ ), i.e.,  $\text{card}\left(\{(i, j) : |\tilde{P}_{ij}| > \epsilon, 1 \leq i \neq j \leq n\}\right)/(n^2 - n)$ , where  $\tilde{P}_{ij} = P_{ij}^*/\max\{|P_{ij}^*| : 1 \leq i \neq j \leq n\}$ .

For comparison, we report the same quantities for the covariance matrices. Results are shown in Table 2.1. This shows the effect of *infill asymptotics* ([8]) on the screen effect, that is, in a fixed domain as  $n$  increases, precision matrices get closer to sparse matrices, but note how the covariance matrices become closer to sparse at a much slower rate.

b) The second motivation for our approach comes from the recent optimization literature on the Sparse Covariance Selection (SCS) problem, first studied by [10] who used the sparsity property of the precision matrix to simplify the covariance structure of a multivariate normal distribution. Given a sample covariance matrix  $S \in \mathbb{R}^{n \times n}$  of a zero-mean multivariate normal random vector  $\mathbf{y} \in \mathbb{R}^n$ , the SCS problem in [9] proposed

Table 2.1: Effect of increasing  $n$  on the near-sparsity of precision matrices (**left**) and covariance matrices (**right**), estimated from a simulated Matern GRF ( $\nu = 3/2$ ) with three different densities of points over a  $100 \times 100$  fixed spatial domain. The numbers are the percentages of nonzero elements in the truncated precision matrices (see the text).

| % of elements s.t. $ \tilde{P}_{ij}  > \epsilon$ |       |      |      | % of elements s.t. $ \tilde{C}_{ij}  > \epsilon$ |       |       |       |
|--|-------|------|------|--|-------|-------|-------|
| $n$  |       |      |      | $n$  |       |       |       |
| $\epsilon$                                       | 10    | 100  | 1000 | $\epsilon$                                       | 10    | 100   | 1000  |
| 0.1  | 10.49 | 0.29 | 0.00 | 0.1  | 16.82 | 13.00 | 12.94 |
| 0.01   | 26.94 | 2.52 | 0.03 | 0.01   | 36.84 | 32.31 | 32.18 |
| 0.001  | 46.46 | 9.34 | 0.28 | 0.001  | 56.86 | 53.04 | 52.86 |

to estimate the corresponding precision matrix by solving a regularized maximum likelihood problem:

$$\min_{P \succ 0} \langle S, P \rangle - \log \det(P) + \alpha \text{card}(P), \quad (2.1)$$

where  $\alpha$  is a given trade-off parameter,  $\text{card}(P)$  denotes the cardinality of non-zero elements  $P$ ,  $\langle \cdot, \cdot \rangle$  denotes the inner product  $\langle S, P \rangle := \text{tr}(S^T P) = \sum_{i,j} S_{ij} P_{ij}$ , and the feasible region for  $P$  is the cone of symmetric, positive definite (PD) matrices denoted by  $P \succ 0$ . The above problem is combinatorially hard due to existence of the cardinality operator in the objective function. A convex approximation of the above problem can be written as

$$\min_{P \succ 0} \langle S, P \rangle - \log \det(P) + \alpha \|P\|_1 \quad (2.2)$$

where the  $\ell_1$  norm is defined as  $\|P\|_1 := \sum_{1 \leq i,j \leq n} |P_{ij}|$  and is the tightest convex envelope of  $\text{card}(\cdot)$ . The large growth of interest in SCS in the last decade is mainly due to the development of powerful first-order algorithms that can deal with  $\ell_1$ -regularized convex optimization problems [9, 45, 14, 31, 23].

c) Our proposed method is also partially related to work that approximates a GRF with a GMRF. This includes the important recent work by [28] who established conditions under which a Matern GRF is exactly Markovian, and provided a way to approximate this GRF with a basis function expansion based on a triangulation in  $\mathbb{R}^d$  where the weights of the expansion obey a GMRF with a specific precision matrix. Earlier methods along this line of work include the classic work of [3] on spatial statistics: a GRF process on a *lattice* (when the locations form a regular lattice) form a Gaussian Markov Random Field (GMRF) under the conditional independence assumption. Lattice GMRF models assume that, given the variables located at the neighboring points of each variable on the lattice, each variable on the lattice is conditionally independent of each other [35]. While the index set has countably finite elements for the lattice data, the index set  $\mathbf{x}$  of a GRF belongs to a continuous set  $\mathcal{X}$ , and this prevents the use of a GMRF model to represent a GRF *exactly*. [38] further elaborate on the concept of a Markovian GRF process in  $d > 1$ . For a finite set of variables generated from a Markovian Matern GRF, the precision matrix will not be sparse, and an exact equivalence between a GMRF and a GRF is not possible. However, given the significant computational advantage when estimating a GMRF over a GRF, especially when  $n$  is large, many authors have attempted to approximate a GRF with a GMRF and this approximation implies the obtained precision matrix is sparse, e.g., [36, 35, 28].

The main idea behind our approach is to approximate *any* GRF by a GMRF *without* using a triangulation of the input space (as proposed by [28]) or assuming a lattice process. Instead, we let the data determine the near-conditional independence pattern between variables corresponding to a finite set of locations in the domain and employ a weighted  $\ell_1$ -regularization similar to that used in the SCS problem to retrieve the independence pattern implicitly through the estimated precision matrix. Although this is a convex problem in the precision matrix variable  $P \in \mathbb{R}^{n \times n}$ , the dimension increases with the number of observations; hence, making the estimation computationally harder as we require matrix inversions with  $\mathcal{O}(n^3)$  complexity at each iteration. For this reason, we propose an additional blocking scheme for large data sets (see section 3).

d) A further motivation for the proposed method is that the spatial locations of the observations are known, and can be utilized for better estimation of the precision matrix. While the number of samples at each location is assumed equal to 1 which implies a rank-*one* sample covariance matrix with low information in (2.2), this can be compensated by making use of the distance information. Indeed, for all different stationary covariance functions tested, we observed that  $|P_{ij}^*|$  decreases to 0 exponentially as  $\|\mathbf{x}_i - \mathbf{x}_j\|_2$  increases, see Figure 2.2.

It is difficult to model the precisions as a function of pairwise distances since each entry in the precision matrix depends on all the entries of the covariance matrix. However, the distance information can be utilized efficiently in penalizing the likelihood function and obtaining a better estimation of the precision matrix (see Section 3.1).

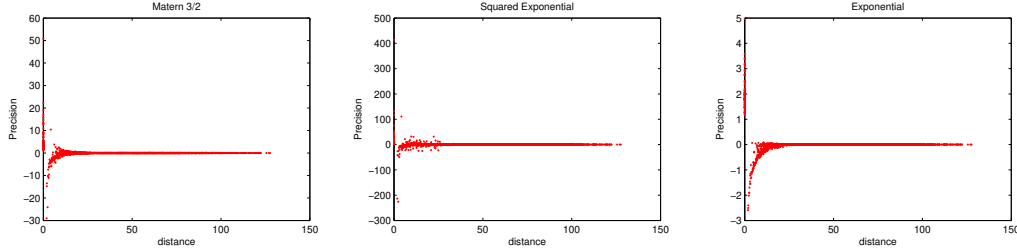


Fig. 2.2: Elements of precision matrices from three covariance functions as a function of the Euclidean distance between the data points. The variance, range, and nugget parameters of the covariance functions are 1, 10, and 0, respectively.

**3. Sparse Precision matrix Selection algorithm for fitting a GRF model.** The proposed SPS method for fitting a GRF is composed of two stages: 1) a sparse precision matrix corresponding to the training data set is estimated by solving a convex maximum likelihood semi-definite program regularized with weighted  $\ell_1$ -norm; 2) after inverting the fitted precision matrix found in the first stage, a least-squares problem is solved to find the parameters of the covariance function.

To perform the first-optimization efficiently for large  $n$ , we propose to partition the set of training locations  $\mathcal{D}^x := \{\mathbf{x}_i\}_{i=1}^n \subset \mathcal{X}$  into  $K$  blocks  $\{\mathcal{D}_k^x\}_{k=1}^K$  of size  $n_k := \text{card}(\mathcal{D}_k^x)$  such that the number of data points in each block  $n_k$  is less than  $n_B$  (in our experiments we set  $n_B$  to 2000). If  $n \leq n_B$ , then blocking is not needed. It is important to note that our SPS method naturally provides a predicted surface with *no* discontinuities at the boundary points between blocks. This is in contrast to other methods that partition large datasets for fitting a GRF which require further formulation to achieve continuity, see [34]. We used the following two blocking schemes in our numerical experiments.

1. **Spatial Segmentation (SS):** This blocking scheme is based on partitioning the spatial domain  $\mathcal{X}$  into  $K$  hypercubes and considering the training data points in each hypercube  $\mathcal{X}_k$  as one block. Let  $\mathcal{X}_k := \{x \in \mathbb{R}^d : \bar{\ell}_k \leq x \leq \bar{u}_k\}$  for some  $\{\bar{\ell}_k, \bar{u}_k\}_{k=1}^K$  such that  $\cup_{k=1}^K \mathcal{X}_k = \mathcal{X}$  and  $\mathcal{X}_{k_1} \cap \mathcal{X}_{k_2} = \emptyset$  for all  $k_1 \neq k_2$ . Then we define  $\mathcal{D}_k^x := \mathcal{D}^x \cap \mathcal{X}_k$  for all  $k$ . Assuming that sample data point locations are uniformly distributed within  $\mathcal{X}$ , each block  $\mathcal{D}_k^x$  will contain the same number of observations in expectation ( $\approx \frac{n}{K}$ ).
2. **Random Selection (RS):** The set of training data locations  $\mathcal{D}^x$  is partitioned *uniformly at random* into  $K$  blocks  $\{\mathcal{D}_k^x\}_{k=1}^K$  such that the first  $K-1$  blocks contain  $\lfloor \frac{n}{K} \rfloor$  data locations and the last block contains  $n - (K-1)\lfloor \frac{n}{K} \rfloor$  data locations.

Let  $\mathcal{D}_k^x = \{(\mathbf{x}_i, y_i) : i \in \mathcal{I}_k\}$  denote the subset of training data corresponding to  $k$ -th block, where the index set  $\mathcal{I}_k$  is defined as  $\mathcal{I}_k := \{1 \leq i \leq n : \mathbf{x}_i \in \mathcal{D}_k^x\}$ . Hence,  $n_k = |\mathcal{I}_k|$ . In the next subsection, we discuss the convex optimization problem solved to estimate  $K$  precision matrices (note how this can be done *in parallel*, if multiple processing units are available).

**3.1. STAGE I: Estimation of precision matrices.** For each block  $k$ , the sample covariance matrix  $S_k \in \mathbb{R}^{n_k \times n_k}$  is calculated as

$$(S_k)_{ij} = (y_i - \mu)(y_j - \mu), \quad \forall (i, j) \in \mathcal{I}_k \times \mathcal{I}_k, \quad (3.1)$$

where  $\mu = \frac{1}{n} \sum_{i=1}^n y_i$ . The corresponding Euclidean pairwise distance matrix  $G_k \in \mathbb{R}^{n_k \times n_k}$  for each block  $k$  is formed as follows: for all  $(i, j) \in \mathcal{I}_k \times \mathcal{I}_k$ ,

$$(G_k)_{ij} = \|\mathbf{x}_i - \mathbf{x}_j\|_2, \quad \text{if } i \neq j, \quad (3.2)$$

$$(G_k)_{ii} = \min\{\|\mathbf{x}_i - \mathbf{x}_j\|_2 : j \in \mathcal{I}_k \setminus \{i\}\}. \quad (3.3)$$

To estimate the precision matrix corresponding to block  $k$ , we propose to solve the following convex program:

$$\hat{P}_k = \underset{P \succ 0}{\operatorname{argmin}} \langle S_k, P \rangle - \log \det(P) + \alpha_k \langle G_k, |P| \rangle, \quad (3.4)$$

where  $|\cdot|$  is the element-wise absolute value operator; hence, the last term is a weighted  $\ell_1$ -norm with weights equal the “distances”  $(G_k)_{ij}$ . Note that  $\hat{P}_k$  is always a full rank matrix due to  $\log \det(P)$  term in the objective function.

In comparison to the covariance selection problem in (2.2), our model (3.4) penalizes each element of the precision matrix with a different weight proportional to the distance between the corresponding locations. In particular, given  $(i, j) \in \mathcal{I}_k \times \mathcal{I}_k$  such that  $i \neq j$ , the penalty weight corresponding to  $(ij)^{th}$ -element is equal to  $\|\mathbf{x}_i - \mathbf{x}_j\|_2$ . This model assumes that the off-diagonal precision magnitudes decrease with distance, for which there is an empirical evidence as shown in Figure 2.2. Moreover, the reason we solve (3.4) using  $G_k$  with strictly positive diagonal is that otherwise the diagonal elements of the precision matrix would not be penalized and they might attain relatively large positive values.

To solve problem (3.4), we propose to use the Alternating Direction Method of Multipliers (ADMM) – see [6]. In order to discuss details of the ADMM algorithm implemented in this paper, consider a more generic problem of the following form:

$$\min_{P \in \mathbb{S}^n} \Psi(P) + \Phi(P), \quad (3.5)$$

where  $\Psi : \mathbb{S}^n \rightarrow \mathbb{R} \cup \{+\infty\}$  and  $\Phi : \mathbb{S}^n \rightarrow \mathbb{R} \cup \{+\infty\}$  are proper closed convex functions, and  $\mathbb{S}^n$  denotes the vector space of  $n$ -by- $n$  symmetric matrices. Given  $\lambda > 0$ , define the prox mapping  $\mathbf{prox}_{\lambda\Psi} : \mathbb{S}^n \rightarrow \mathbb{S}^n$  as follows:

$$\mathbf{prox}_{\lambda\Psi}(\bar{P}) = \underset{P \in \mathbb{S}^n}{\operatorname{argmin}} \lambda\Psi(P) + \frac{1}{2}\|P - \bar{P}\|_F^2, \quad (3.6)$$

where  $\|\cdot\|_F$  denotes the Frobenius norm. The prox mapping  $\mathbf{prox}_{\lambda\Phi} : \mathbb{S}^n \rightarrow \mathbb{S}^n$  is defined similarly. Suppose that minimizing (3.5) in  $P \in \mathbb{S}^n$  is not an easy task but  $\mathbf{prox}_{\lambda\Psi}$  and  $\mathbf{prox}_{\lambda\Phi}$  maps can be computed efficiently for all  $\lambda > 0$ . By introducing an auxiliary variable  $Z \in \mathbb{S}^n$ , (3.5) can be equivalently written as  $\min\{\Psi(P) + \Phi(Z) : P = Z, P, Z \in \mathbb{S}^n\}$ . Next, for a given penalty parameter  $\rho > 0$ , the augmented Lagrangian function is defined as

$$\mathcal{L}_\rho(P, Z, W) := \Psi(P) + \Phi(Z) + \langle W, P - Z \rangle + \frac{\rho}{2}\|P - Z\|_F^2, \quad (3.7)$$

where  $W \in \mathbb{S}^n$  is the dual multiplier for the linear constraint  $P - Z = \mathbf{0}$ .

Given a penalty sequence  $\{\rho_\ell\}_{\ell \geq 1} \subset \mathbb{R}_{++}$  and an initial primal-dual point  $Z^1, W^1 \in \mathbb{S}^n$ , ADMM solves (3.5) by computing a sequence of iterates  $\{P_\ell, Z_\ell\}_{\ell \geq 1}$  according to:

$$P_{\ell+1} = \underset{P \in \mathbb{S}^n}{\operatorname{argmin}} \mathcal{L}_{\rho_\ell}(P, Z_\ell, W_\ell) = \mathbf{prox}_{\Psi/\rho_\ell} \left( Z_\ell - \frac{1}{\rho_\ell} W_\ell \right), \quad (3.8a)$$

$$Z_{\ell+1} = \underset{Z \in \mathbb{S}^n}{\operatorname{argmin}} \mathcal{L}_{\rho_\ell}(P_{\ell+1}, Z, W_\ell) = \mathbf{prox}_{\Phi/\rho_\ell} \left( P_{\ell+1} + \frac{1}{\rho_\ell} W_\ell \right), \quad (3.8b)$$

$$W_{\ell+1} = W_\ell + \rho_\ell (P_{\ell+1} - Z_{\ell+1}). \quad (3.8c)$$

The iterative algorithm above is terminated at the end of iteration  $\ell$  when both primal and dual residuals  $(r_\ell, s_\ell)$  are below a given tolerance value, where  $r_\ell := P_{\ell+1} - Z_{\ell+1}$  and  $s_\ell := \rho_\ell(Z_{\ell+1} - Z_\ell)$ . Indeed, necessary and sufficient optimality conditions for (3.8a) and (3.8b) imply that when  $r_\ell = s_\ell = 0$ ,  $P_{\ell+1} = Z_{\ell+1}$  is the optimal solution to (3.5). In practice, it is often the case, as in our numerical experiments, that ADMM converged to an acceptable accuracy within a few tens of iterations.

For all  $\rho > 0$ , convergence of the ADMM iterate sequence  $\{P_\ell, Z_\ell\}_{\ell \geq 1}$  is guaranteed when the penalty parameter is held constant equal to  $\rho$ , i.e.  $\rho_\ell = \rho > 0$  for all  $\ell \geq 1$ . In particular,  $\lim_{\ell \geq 1} Z_\ell = \lim_{\ell \geq 1} P_\ell$ ; moreover, any limit point of  $\{P_\ell\}$  is a minimizer of (3.5). For details on the convergence of constant penalty ADMM algorithms see [6, 12, 13] and on the convergence of variable penalty ADMM algorithms see [20, 21, 1, 25, 6]. Recently, [11] showed that constant penalty ADMM iterate sequence converges linearly if  $\Psi$  is strongly convex and has a Lipschitz continuous gradient. In particular,  $\{P_\ell, W_\ell\}$  sequence converges<sup>2</sup>  $Q$ -linearly to a primal-dual optimal pair  $(P^{\text{opt}}, W^{\text{opt}})$  with  $P^{\text{opt}}$  being unique; and  $\{Z_\ell\}$  sequence converges  $R$ -linearly to  $P^{\text{opt}}$ .

Returning to the SPS method, we note that the precision matrix estimation problem for the  $k$ -th block given in (3.4) immediately fits into the ADMM framework by setting  $\Psi(P) = \langle S_k, P \rangle - \log \det(P) + \mathbf{1}_{\mathcal{Q}_k}(P)$  and  $\Phi(P) = \alpha_k \langle G_k, |P| \rangle$ , where  $\mathcal{Q}_k := \{P \in \mathbb{S}^{n_k} : P \succ \mathbf{0}\}$  and  $\mathbf{1}_{\mathcal{Q}_k}(\cdot)$  is the indicator function of  $\mathcal{Q}_k$ , i.e.  $\mathbf{1}_{\mathcal{Q}_k}(P) = 0$  if  $P \in \mathcal{Q}_k$ ; and it is equal to  $+\infty$ , otherwise. Therefore, both  $\Psi$  and  $\Phi$  are indeed closed convex functions. Indeed,  $\Psi$  is strictly convex and differentiable on  $\mathcal{Q}_k$  with  $\nabla \Psi(P) = S_k - P^{-1}$ ; however, note that  $\nabla \Psi(P)$  is not Lipschitz continuous on  $\mathcal{Q}_k$ . Therefore, this choice of  $\Psi$  and  $\Phi$  do not satisfy the assumptions in [11]. On the other hand, following the discussion in [9], we will show that by selecting a slightly different  $\mathcal{Q}_k$ , one can obtain an equivalent problem to (3.4) which does satisfy the ADMM convergence assumptions in [11]. Hence, we show next that with the ADMM algorithm, we enjoy a linear convergence rate for stage I of the SPS method.

Noting that  $|t| = \max\{ut : |u| \leq 1\}$ , one can write (3.4) equivalently as follows:

$$\hat{F}_k := \min_{P \succ \mathbf{0}} \max_{\{U \in \mathbb{S}^{n_k} : |U_{ij}| \leq \alpha_k(G_k)_{ij}\}} \mathcal{L}(P, U) := \langle S_k + U, P \rangle - \log \det(P), \quad (3.9)$$

where  $\hat{F} := \langle S_k, \hat{P}_k \rangle - \log \det(\hat{P}_k) + \alpha_k \langle G_k, |\hat{P}_k| \rangle$ . Since  $\mathcal{L}$  is convex in  $P$ , linear in  $U$ , and  $\{U \in \mathbb{S}^{n_k} : |U_{ij}| \leq \alpha_k(G_k)_{ij}\}$  is compact, the strong min-max property holds:

$$\hat{F}_k = \max_{\{U \in \mathbb{S}^{n_k} : |U_{ij}| \leq \alpha_k(G_k)_{ij}\}} \min_{P \succ \mathbf{0}} \mathcal{L}(P, U), \quad (3.10)$$

$$= \max_{\{U \in \mathbb{S}^{n_k} : |U_{ij}| \leq \alpha_k(G_k)_{ij}\}} n_k - \log \det((S_k + U)^{-1}), \quad (3.11)$$

where (3.11) follows from the fact that for a given  $U \in \mathbb{S}^{n_k}$ ,  $\hat{P}(U) = (S_k + U)^{-1}$  minimizes the inner problem in (3.10) if  $S_k + U \succ \mathbf{0}$ ; otherwise, the inner minimization problem is unbounded from below. Therefore, we conclude that  $\hat{P}_k$  is the optimal solution to (3.4) if and only if there exists  $\hat{U} \in \mathbb{S}^{n_k}$  such that  $\hat{P}_k = (S_k + \hat{U})^{-1} \succ \mathbf{0}$ ,  $|\hat{U}_{ij}| \leq \alpha_k(G_k)_{ij}$  for all  $(i, j) \in \mathcal{I}_k$ , and  $\langle S_k, \hat{P}_k \rangle + \alpha_k \langle G_k, |\hat{P}_k| \rangle = n_k$ . From these optimality conditions, it follows

$$a_k := \frac{1}{\|S_k\|_2 + \alpha_k \|G_k\|_F} \leq \frac{1}{\|S_k\|_2 + \|\hat{U}\|_F} \leq \frac{1}{\|S_k + \hat{U}\|_2} = \sigma_{\min}(\hat{P}_k), \quad (3.12)$$

$$b_k := \frac{n_k}{\alpha_k c_k} \geq \frac{\langle G_k, |\hat{P}_k| \rangle}{c_k} \geq \sum_{i,j} |(\hat{P}_k)_{ij}| \geq \|\hat{P}_k\|_F \geq \|\hat{P}_k\|_2 = \sigma_{\max}(\hat{P}_k), \quad (3.13)$$

where  $c_k := \min\{G_{ij} : (i, j) \in \mathcal{I}_k \times \mathcal{I}_k, i \neq j\} > 0$ . Therefore, we can conclude that there exist  $0 < a_k \leq b_k < \infty$  such that  $a_k \mathbf{I} \preceq \hat{P}_k \preceq b_k \mathbf{I}$ . Hence, (3.4) is equivalent to

$$\hat{P}_k = \operatorname{argmin}\{\langle S_k, P \rangle - \log \det(P) + \alpha_k \langle G_k, |P| \rangle : a_k \mathbf{I} \preceq P \preceq b_k \mathbf{I}\}, \quad (3.14)$$

---

<sup>2</sup>Let  $\{X_\ell\}$  converge to  $X^*$  for a given norm  $\|\cdot\|$ . The convergence is called  $Q$ -linear if  $\frac{\|X_{\ell+1} - X^*\|}{\|X_\ell - X^*\|} \leq c$ , for some  $c \in (0, 1)$ ; and  $R$ -linear if  $\|X_\ell - X^*\| \leq c_\ell$ , for some  $\{c_\ell\}$  converging to 0  $Q$ -linearly.



for  $a_k$  and  $b_k$  defined in (3.12) and (3.13), respectively. It is important to note that one can also exploit the prior information on the process to obtain more accurate estimates on the  $a_k$  and  $b_k$  parameters of formulation (3.14). For instance, let  $C_k^f(\theta_1^*, \theta_2^*) + \theta_0^* \mathbf{I}$  be the covariance matrix corresponding to locations in  $\mathcal{D}_k^x$ , and  $P_k^*$  denote its inverse, where  $\theta_1^*$  and  $\theta_2^*$  denote the true variance and range parameters of the process. The common structure of the covariance functions imply that  $\text{diag}(C_k^f(\theta_1^*, \theta_2^*)) = \theta_1^* \mathbf{1}$ , where  $\mathbf{1}$  denotes the vector of ones. Therefore, we can conclude that  $\sigma_{\min}(P_k^*) \geq 1/\text{Tr}(C_k^f(\theta_1^*, \theta_2^*) + \theta_0^* \mathbf{I}) = \frac{1}{n_k(\theta_0^* + \theta_1^*)}$ . Hence, if lower bounds on  $\theta_0^*$  and  $\theta_1^*$  are known apriori, then we might obtain a tighter lower bound than the one given in (3.12).

Going back to the convergence rate discussion, when ADMM is applied to (3.14) we can guarantee that the primal-dual iterate sequence converges linearly. In particular, we apply ADMM on (3.5) with

$$\Psi(P) = \langle S_k, P \rangle - \log \det(P) + \mathbf{1}_{\mathcal{Q}_k}(P), \quad \mathcal{Q}_k := \{P \in \mathbb{S}^{n_k} : a_k \mathbf{I} \preceq P \preceq b_k \mathbf{I}\}, \quad (3.15)$$

$$\Phi(P) = \alpha_k \langle G_k, |P| \rangle + \mathbf{1}_{\mathcal{Q}'_k}(P), \quad \mathcal{Q}'_k := \{P \in \mathbb{S}^{n_k} : \text{diag}(P) \geq \mathbf{0}\}. \quad (3.16)$$

Since  $\mathcal{Q}_k \subset \mathbb{S}_+^{n_k} \subset \mathcal{Q}'_k$ , the term  $\mathbf{1}_{\mathcal{Q}'_k}(\cdot)$  in the definition of  $\Phi$  appears redundant. However, defining  $\Phi$  this way will restrict the sequence  $\{Z_\ell\}$  to lie in  $\mathcal{Q}'_k$ , which leads to faster convergence to feasibility in practice. By resetting  $\mathcal{Q}_k$  as in (3.15), we ensure that  $\Psi$  is strongly convex with constant  $1/b_k^2$  and  $\nabla \Psi$  is Lipschitz continuous with constant  $1/a_k^2$ . Indeed, the Hessian of  $\Psi$  is a quadratic form on  $\mathbb{S}^{n_k}$  such that  $\nabla^2 \Psi(P)[H, H] = \text{Tr}(P^{-1} H P^{-1} H)$ , which implies  $\frac{1}{b_k^2} \|H\|_F^2 \leq \nabla^2 \Psi(P)[H, H] \leq \frac{1}{a_k^2} \|H\|_F^2$ .

Note that in every ADMM iteration shown in (3.8), one needs to compute  $\text{prox}_{\Psi/\rho}$  and  $\text{prox}_{\Phi/\rho}$ . Next, we show that these maps can be written in closed form.

LEMMA 3.1. *Let  $\Phi : \mathbb{S}^{n_k} \rightarrow \mathbb{R}$  be defined as in (3.16). For given  $\bar{P} \in \mathbb{S}^{n_k}$  and  $\rho > 0$ , one has*

$$(\text{prox}_{\Phi/\rho}(\bar{P}))_{ij} = \text{sgn}(\bar{P}_{ij}) \max \left\{ |\bar{P}_{ij}| - \frac{\alpha_k}{\rho} (G_k)_{ij}, 0 \right\}, \quad \forall (ij) \in \mathcal{I}_k \times \mathcal{I}_k \text{ s.t. } i \neq j, \quad (3.17a)$$

$$(\text{prox}_{\Phi/\rho}(\bar{P}))_{ii} = \max \left\{ \bar{P}_{ii} - \frac{\alpha_k}{\rho} (G_k)_{ii}, 0 \right\}, \quad \forall i \in \mathcal{I}_k. \quad (3.17b)$$

*Proof.* From the definition of  $\text{prox}_{\Phi/\rho}$ , we have

$$\text{prox}_{\Phi/\rho} = \underset{P \in \mathbb{S}^{n_k}}{\text{argmin}} \left\{ \sum_{(i,j) \in \mathcal{I}_k \times \mathcal{I}_k} \frac{\alpha_k}{\rho} (G_k)_{ij} |P_{ij}| + \frac{1}{2} |P_{ij} - \bar{P}_{ij}|^2 : \text{diag}(P) \geq \mathbf{0} \right\}. \quad (3.18)$$

For a given  $\bar{t} \in \mathbb{R}$ , and  $\gamma > 0$ , the unique minimizer of  $\min_{t \in \mathbb{R}} \gamma |t| + \frac{1}{2} |t - \bar{t}|^2$  can be written as  $\text{sgn}(\bar{t}) \max\{|\bar{t}| - \gamma, 0\}$ ; and the unique minimizer of  $\min_{t \in \mathbb{R}} \{\gamma t + \frac{1}{2} |t - \bar{t}|^2 : t \geq 0\}$  can be written as  $\max\{\bar{t} - \gamma, 0\}$ . Hence, (3.17) follows from the separability of the objective function in (3.18).  $\square$

LEMMA 3.2. *Let  $\Psi : \mathbb{S}^{n_k} \rightarrow \mathbb{R}$  be defined as in (3.15). For given  $\bar{P} \in \mathbb{S}^{n_k}$  and  $\rho > 0$ , one has  $\text{prox}_{\Psi/\rho}(\bar{P}) = U \text{diag} \lambda^* U^T$  and*

$$\lambda_i^* = \max \left\{ \min \left\{ \frac{\bar{\lambda}_i + \sqrt{\bar{\lambda}_i^2 + 4\rho}}{2\rho}, b_k \right\}, a_k \right\}, \quad i = 1, \dots, n_k, \quad (3.19)$$

where  $\bar{P} - \frac{1}{\rho} S_k$  has the eigen-decomposition  $U \text{diag}(\bar{\lambda}) U^T$ .

*Proof.* The  $\text{prox}_{\Psi/\rho}$  map can be equivalently written as

$$\text{prox}_{\Psi/\rho}(\bar{P}) = \underset{P \in \mathbb{S}^{n_k}}{\text{argmin}} \{ -\log \det(P) + \frac{\rho}{2} \|P - (\bar{P} - \frac{1}{\rho} S_k)\|_F^2 : a_k \mathbf{I} \preceq P \preceq b_k \mathbf{I} \}. \quad (3.20)$$

Let  $U \text{diag}(\bar{\lambda}) U^T$  be the eigen-decomposition of  $\bar{P} - \frac{1}{\rho} S_k$ . Fixing  $U \in \mathbb{S}^{n_k}$ , and by restricting the variable  $P \in \mathbb{S}^{n_k}$  in (3.20) to have the form  $U \text{diag}(\lambda) U^T$  for some  $\lambda \in \mathbb{R}^{n_k}$ , we obtain the optimization problem (3.21) over the variable  $\lambda \in \mathbb{R}^{n_k}$ :

$$\min_{\lambda \in \mathbb{R}^{n_k}} \left\{ -\sum_{i=1}^{n_k} \log(\lambda_i) + \frac{\rho}{2} (\lambda_i - \bar{\lambda}_i)^2 : a_k \leq \lambda_i \leq \beta_k, i = 1, \dots, n_k \right\}. \quad (3.21)$$

For a given  $\bar{t} \in \mathbb{R}$ , and  $a, b, \gamma > 0$ , the unique minimizer of  $\min_{t \in \mathbb{R}} \{-\log(t) + \frac{\rho}{2}|t - \bar{t}|^2 : a \leq t \leq b\}$  can be written as  $\max \left\{ \min \left\{ \frac{\bar{t} + \sqrt{\bar{t}^2 + 4\rho}}{2\rho}, b \right\}, a \right\}$ . Hence,  $\lambda^* \in \mathbb{R}^{n_k}$  given in (3.19) is the unique minimizer of (3.21). Let  $h : \mathbb{R}^{n_k} \rightarrow \mathbb{R} \cup \{+\infty\}$  be defined as  $h(\lambda) := -\sum_{i=1}^{n_k} \log(\lambda_i) + \mathbf{1}_{\mathcal{H}_k}(\lambda)$ , where  $\mathcal{H}_k := \{\lambda \in \mathbb{R}^{n_k} : a_k \mathbf{1} \leq \lambda \leq b_k \mathbf{1}\}$  for  $a_k$  and  $b_k$  defined in (3.12) and (3.13). Hence,  $\lambda^* = \operatorname{argmin}_{\lambda \in \mathbb{R}^{n_k}} \{h(\lambda) + \frac{\rho}{2}\|\lambda - \bar{\lambda}\|_2^2\}$ . Therefore, from the first-order optimality conditions, it follows that

$$\bar{\lambda} - \lambda^* \in \frac{1}{\rho} \partial h(\lambda)|_{\lambda=\lambda^*}. \quad (3.22)$$

Let  $H : \mathbb{S}^{n_k} \rightarrow \mathbb{R} \cup \{+\infty\}$  be such that  $H(P) = -\log \det(P) + \mathbf{1}_{\mathcal{Q}_k}(P)$ . Definition of  $\mathbf{prox}_{\Psi/\rho}(\bar{P})$  implies that  $\rho \left( \bar{P} - \frac{1}{\rho} S_k - \mathbf{prox}_{\Psi/\rho}(\bar{P}) \right) \in \partial H(P)|_{P=\mathbf{prox}_{\Psi/\rho}(\bar{P})}$ . In the rest of the proof,  $\sigma : \mathbb{S}^{n_k} \rightarrow \mathbb{R}^{n_k}$  denotes the function that returns the singular values of its argument. Note that  $H(P) = h(\sigma(P))$  for all  $P \in \mathbb{S}^{n_k}$ . Since  $f$  is *absolutely symmetric*, Corollary 2.5 in [26] implies that  $P^{\text{prox}} = \mathbf{prox}_{\Psi/\rho}(\bar{P})$  if and only if  $\sigma(\bar{P} - \frac{1}{\rho} S_k - P^{\text{prox}}) \in \frac{1}{\rho} \partial h(\lambda)|_{\lambda=\sigma(P^{\text{prox}})}$  and there exists a simultaneous singular value decomposition of the form  $P^{\text{prox}} = U \operatorname{diag}(\sigma(P^{\text{prox}})) U^T$  and  $\bar{P} - \frac{1}{\rho} S_k - P^{\text{prox}} = U \operatorname{diag} \left( \sigma \left( \bar{P} - \frac{1}{\rho} S_k - P^{\text{prox}} \right) \right) U^T$ . Hence, it follows from (3.22) that  $\mathbf{prox}_{\Psi/\rho}(\bar{P}) = U \operatorname{diag}(\lambda^*) U^T$ .  $\square$

In ADMM algorithms [6, 12, 13], the penalty parameter is typically held constant, i.e.  $\rho_\ell = \rho > 0$  for all  $\ell \geq 1$ , for some  $\rho > 0$ . Although convergence of ADMM is guaranteed for all  $\rho > 0$ , the empirical performance of ADMM algorithms critically depend on the choice of penalty parameter  $\rho$  - it deteriorates rapidly if the penalty is set too large or too small [16, 18, 25]. Moreover, it is discussed in [29] that there exists  $\rho^* > 0$  which optimizes the convergence rate for the constant penalty ADMM scheme; however, estimating  $\rho^*$  is difficult in practice [21]. In our experiments, we used an increasing penalty sequence  $\{\rho_\ell\}_{\ell \geq 1}$ . For details on the convergence of variable penalty ADMM algorithms see [20, 21, 1, 25, 6].

---

**Algorithm 1** Sparse Precision matrix Selection (SPS)

---

**input:**  $\mathcal{D} = \{(\mathbf{x}_i, y_i)\}_{i=1}^n \subset \mathcal{X} \times \mathbb{R}$ ,  $n_B$   
 $\mu \leftarrow \frac{1}{n} \sum_{i=1}^n y_i$ ,  $K \leftarrow \left\lceil \frac{n}{n_B} \right\rceil$   
/\* Segmentation: split data into  $K$  blocks – See section 3\*/  
 $\{\mathcal{I}_k\}_{k=1}^K$  is a partition of  $\{1, \dots, n\}$   
/\* Compute sample covariance matrices \*/  
**for**  $k \leftarrow 1$  **to**  $K$  **do**  
     $(S_k)_{ij} \leftarrow (y_i - \mu)(y_j - \mu)$ ,  $\forall (i, j) \in \mathcal{I}_k \times \mathcal{I}_k$   
     $(G_k)_{ij} \leftarrow \|\mathbf{x}_i - \mathbf{x}_j\|_2$ ,  $\forall (i, j) \in \mathcal{I}_k \times \mathcal{I}_k$   
     $(G_k)_{ii} \leftarrow \min\{\|\mathbf{x}_i - \mathbf{x}_j\|_2 : j \in \mathcal{I}_k \setminus \{i\}\}$ ,  $\forall i \in \mathcal{I}_k$   
**end for**  
/\* Compute fitted precision matrices – See Section 3.1 \*/  
**for**  $k \leftarrow 1$  **to**  $K$   
     $\hat{P}_k \leftarrow \operatorname{argmin} \{\langle S_k, P_k \rangle - \log \det(P_k) + \alpha_k \langle G_k, |P_k| \rangle : a_k \mathbf{I} \preceq P_k \preceq b_k \mathbf{I}\}$   
**end for**  
/\* Estimate process parameters – See Section 3.2 \*/  
**if** process is stationary **then**  
     $\hat{\boldsymbol{\theta}} \leftarrow \operatorname{argmin}_{\boldsymbol{\theta} \in \Theta} \sum_{k=1}^K \|\hat{P}_k^{-1} - C_k(\boldsymbol{\theta})\|_F^2$   
**else**  
     $\hat{\boldsymbol{\theta}}_k \leftarrow \operatorname{argmin}_{\boldsymbol{\theta}_k \in \Theta} \|\hat{P}_k^{-1} - C_k(\boldsymbol{\theta}_k)\|_F^2$ ,  $k = 1, \dots, K$   
**end if**  
**return:**  $\hat{\boldsymbol{\theta}}$  or  $\{\hat{\boldsymbol{\theta}}_k\}_{k=1}^K$

---

**3.2. STAGE II: Estimation of covariance function parameters.** After sparse precision matrices have been estimated for each block in the first stage, a least-squares problem is solved in the second stage to fit a covariance function to  $\{\hat{P}_k\}_{k=1}^K$ . Although this is a non-convex problem for parametric covariance functions such as Matern, Squared-Exponential, etc., our numerical results suggest that non-convexity of this problem is much less serious than that of the likelihood function (1.5). For a stationary GRF, the prediction surface generated with this approach will not have any discontinuities at the boundary points between blocks. Indeed, although a different precision matrix is obtained for each block in stage I, a *single* covariance matrix is obtained in stage II over the full domain of the process. Below, we go over the second stage optimization problem for second-order stationary processes, and briefly discuss the modifications needed for non-stationary processes.

Under the assumption that the underlying stochastic process is second-order stationary, i.e., the covariance function parameters are fixed across the domain  $\mathcal{X}$  [40], one can fit a single covariance function for the whole domain. In this case, for both blocking schemes (SS or RS, see section 3), we propose to estimate the covariance function parameters by solving the following least squares problem:

$$\hat{\boldsymbol{\theta}} \in \operatorname{argmin}_{\boldsymbol{\theta} \in \Theta} \sum_{k=1}^K \|\hat{P}_k^{-1} - C_k(\boldsymbol{\theta})\|_F^2, \quad (3.23)$$

where  $C_k(\boldsymbol{\theta})$  is the parametric covariance matrix corresponding to  $\mathcal{D}_k^x$ , the locations of elements in block  $k$ . For isotropic covariance functions with nugget [40], this optimization problem can be reduced to a much simpler *one-dimensional* search in the range parameter as is shown in Appendix A. Indeed, we first minimize (3.23) over  $\theta_1$  (variance parameter) and  $\theta_0$  (nugget parameter), which can be done in closed form – see (A.6) in the appendix. Hence, the non-convex objective in (3.23) can be written as a function of  $\theta_2$  (range parameter) *only*. Next, we minimize it over  $0 \leq \theta_2 \leq D_{\max}$  to get  $\hat{\theta}_2$ , where  $D_{\max} = \max\{\|\mathbf{x} - \mathbf{x}'\|_2 : \mathbf{x}, \mathbf{x}' \in \mathcal{X}\}$ . Figure 3.1 shows the shape of the objective function of the second stage optimization as a function of  $\theta_2$  where the true parameter value  $(\theta_0^*, \theta_1^*, \theta_2^*)^T$  is equal to  $(4, 8, 4)^T$  and the covariance function is the squared exponential. As we can see, the objective function is unimodal with the global minimum *almost* at the true  $\theta_2^*$  value. The univariate minimization is performed via bisection; hence, after  $\log_2(D_{\max}/\epsilon)$  iterations, the algorithm reaches to a point with distance less than  $\epsilon$  from the global minimum.

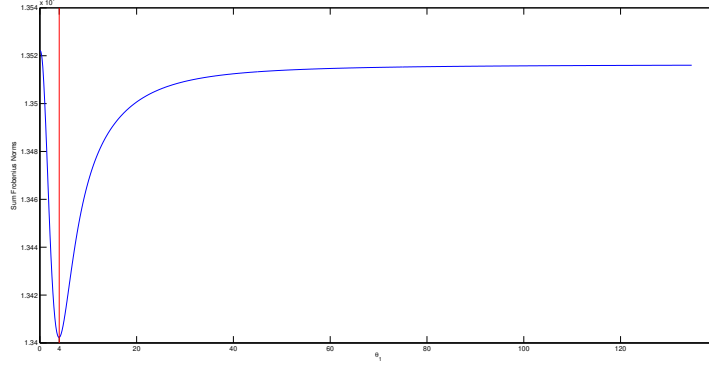


Fig. 3.1: Objective function of the stage II optimization in the proposed SPS method as a function of the range parameter  $\theta_2$ . The red line shows the true value of the range parameter ( $\theta_2^* = 4$ )

In the case where the process is non-stationary, only the SS blocking scheme can be used. Here, the second stage optimization is solved separately for each block, i.e., each block has its own covariance function parameter estimates. The covariance function parameter estimates for each block are computed by solving

$$\hat{\theta}_k \in \underset{\theta_k \in \Theta}{\operatorname{argmin}} \|\hat{P}_k^{-1} - C_k(\theta_k)\|_F^2, \quad k = 1, \dots, K. \quad (3.24)$$

Finally, to predict the process at a new location, the block corresponding to the new location in SS scheme and  $\hat{\theta}_k$  are used in the prediction formula (1.3).

A summary of the proposed Sparse Precision matrix Selection (SPS) method including estimation of the precision matrix and hyper-parameters  $\theta$  is provided in Algorithm 1.

**4. Numerical performance of the proposed SPS method.** In this section, the performance of the proposed algorithm is tested on both simulated and real data sets. Let  $N$  denote the number of simulation replications. For each replication, 90% of the data set is allocated for training (i.e., estimating the hyper-parameters) and 10% for testing (prediction). The performance measure is the Mean Square Prediction Error (MSPE) computed on the *test data*. MSPE corresponding to the  $i$ -th replication is computed as follows:

$$\text{MSPE}^{(i)} = \frac{1}{n_t^{(i)}} \left( \mathbf{y}_t^{(i)} - \hat{\mathbf{y}}_t^{(i)} \right)^T \left( \mathbf{y}^{(i)} - \hat{\mathbf{y}}_t^{(i)} \right), \quad (4.1)$$

where  $n_t^{(i)}$  denotes the number of *test data* points in the  $i$ -th replication,  $\mathbf{y}_t^{(i)}$  and  $\hat{\mathbf{y}}_t^{(i)}$  are  $n_t^{(i)} \times 1$  vectors of true and predicted function values, respectively. Let  $\hat{\theta}^{(i)}$  denote the estimate of covariance parameters obtained using SPS, shown in Algorithm 1, in the  $i$ -th replication. In all the tables in this section,  $\bar{\theta} := \sum_{i=1}^N \hat{\theta}^{(i)} / N$  and  $\text{stdev}_{\theta} := \sqrt{\frac{1}{N} \sum_{i=1}^N (\hat{\theta}^{(i)} - \bar{\theta})^2}$  denote the sample mean and the standard deviation of the parameter estimates, respectively.  $\overline{\text{MSPE}}$  and  $\text{stdev}_{\text{MSPE}}$  are also defined similarly.

**4.1. Prediction performance of SPS-fitted GRF for small and large data sets.** We simulated two data sets of sizes  $n = 1,000$  and  $n = 64,000$  points from a GRF with zero mean and isotropic squared-exponential (SE) covariance function with nugget  $\theta_0^* = 4$ , variance  $\theta_1^* = 8$ , and range  $\theta_2^* = 4$  over a squared domain of size  $100 \times 100$ . Let  $N$  denote the number of replications. In the simulation with  $n = 1000$ , we calculated the mean and standard deviation of the parameter estimates and the MSPE for  $N = 100$  replicates, i.e., we fixed the training data locations  $\mathcal{D}^x \in \mathbb{R}^d$  and hence the distance matrix  $G \in \mathbb{R}^{n \times n}$ . In each replication  $\mathbf{y} \in \mathbb{R}^n$  was sampled from a zero mean GRF with the covariance matrix built from the above covariance function over  $\mathcal{D}^x$ . In the simulation with  $n = 64,000$ , we followed the same procedure; however,

since each run of the simulation takes around 3-4 hours, the means and standard deviations were calculated from  $N=5$  replicates only.

To calculate the MSPE, we randomly selected the test locations, and fixed them across all the replicates. Furthermore, since the true parameter values are known in a simulated data set, the true function values  $\mathbf{y}_t$  are taken to be the predictions obtained via (1.3) using the true parameter values. Calculating the MSPE this way shows the specific error due to the discrepancies between the estimated and true parameter values.

The parameter  $\alpha_k$  in (3.14) was set to  $1/\sqrt{n_k}$  and the penalty sequence  $\{\rho_\ell\}$  of the ADMM given in (3.8) was set to a geometrically increasing sequence  $\rho_{\ell+1} = 1.05\rho_\ell$  with  $\rho_0 = 1$ . Both blocking schemes (SS and RS) were used for comparison purposes. When  $n = 1000$ , for both SS and RS blocking schemes, the domain was split into 9 equal size blocks, i.e.  $n_k$  was set to  $\frac{1}{9}(900) = 100$  for each block (recall that 10% of data points were used for testing). Similarly, when  $n = 64,000$ , for both SS and RS blocking schemes, the domain was split into 64 equal size blocks, i.e.  $n_k$  was set to  $\frac{1}{64}(57600) = 900$  for each block. For details of SS and RS blocking schemes, see Section 3. Table 4.1 shows the model fitting results.

Table 4.1: SPS model estimation results for simulated data sets. The covariance function is SE and the true hyper-parameter values are  $\theta_0^* = 4$ ,  $\theta_1^* = 8$ , and  $\theta_2^* = 4$ .

| Block | $n=1000$ (N=100 replicates)                          |  |                          |                              | $n=64000$ (N=5 replicates)                           |  |                          |                              |
|-------|--|--|--------------------------|------------------------------|--|--|--------------------------|------------------------------|
|       | $\bar{\theta}$                                       | $\text{stdev}_\theta$                                | $\overline{\text{MSPE}}$ | $\text{stdev}_{\text{MSPE}}$ | $\bar{\theta}$                                       | $\text{stdev}_\theta$                                | $\overline{\text{MSPE}}$ | $\text{stdev}_{\text{MSPE}}$ |
| SS    | $\begin{pmatrix} 3.98 \\ 7.77 \\ 4.87 \end{pmatrix}$ | $\begin{pmatrix} 0.41 \\ 1.01 \\ 0.76 \end{pmatrix}$ | 0.1269                   | 0.1468                       | $\begin{pmatrix} 4.01 \\ 8.16 \\ 4.75 \end{pmatrix}$ | $\begin{pmatrix} 0.43 \\ 0.78 \\ 0.29 \end{pmatrix}$ | 0.0381                   | 0.0209                       |
| RS    | $\begin{pmatrix} 3.83 \\ 8.05 \\ 4.64 \end{pmatrix}$ | $\begin{pmatrix} 0.91 \\ 2.36 \\ 2.15 \end{pmatrix}$ | 5.5462                   | 25.8123                      | $\begin{pmatrix} 3.98 \\ 7.97 \\ 4.83 \end{pmatrix}$ | $\begin{pmatrix} 0.06 \\ 0.11 \\ 0.11 \end{pmatrix}$ | 0.0007                   | 0.0009                       |

According to the simulation results, when  $n = 1000$ , the parameter estimates using either blocking scheme appear unbiased while the standard deviations obtained via SS blocking scheme are significantly lower than those obtained using a RS blocking scheme. The mean MSPE and its standard deviations are also considerably better under the SS blocking scheme. This is because in a SS blocking scheme points in one block are independent of the points in another block conditional on all other points even though this assumption is partially violated at the boundary points. In contrast, this conditional independence assumption seems not to be reasonable if points in a block are randomly selected over all the domain as in a RS blocking scheme. However, when  $n = 64,000$ , the larger point density per block makes the assumption of independence between blocks not so relevant, and here parameter estimates under the RS blocking scheme are better estimated and hence the MSPE is also better.

**4.2. Effect of range and nugget parameters.** To analyze the effect of the range ( $\theta_2^*$ ) and nugget ( $\theta_0^*$ ) parameters on the performance of the proposed method, we setup another simulation with  $n=64,000$  points with results shown in Table 4.2. From the table, when the range parameter increases, the standard deviations of the parameter estimates increase under both blocking schemes. Furthermore, the RS scheme appears to be less sensitive to changes in the nugget parameter, but the effects for SS blocking are moderate, mostly observed in the MSPE. In general, given the high point density, the RS blocking scheme comes up with better prediction performance (lower standard deviation of MSPE across the replicates).

**4.3. SPS vs. alternative methods for fitting GRFs to big data sets.** Finally, we tested the performance of our algorithm against some other popular methods for fitting a GRF model to large data sets from the different classes reviewed in Section 1. In particular, we compared our *Sparse Precision matrix Selection* (SPS) method against the *Partial Independent Conditional* (PIC) method by [39], the *Domain Decomposition* (DDM) method of [34], and the *Full Scale covariance Approximation* (FSA) of [37]. [34] provided useful computer codes for PIC and DDM and we coded the FSA method. We simulated a data set of size  $n = 1000$  generated from a zero mean GRF with isotropic Squared-Exponential (SE) covariance function with the following parameter values:  $\theta_0^*=4$  (nugget),  $\theta_1^*=8$  (variance), and  $\theta_2^*=4$  (range). In our SPS method, we used SS blocking scheme with 9 equal-size blocks as described in Section 3. In the PIC

Table 4.2: Result of five replications of the  $n = 64,000$  point simulation with SE covariance function and variance parameter  $\theta_1^*$  equal to 8.

| Nugget           | Block | $\theta_2^* = 4$                                     |  |        |                              | $\theta_2^* = 30$                                     |  |        |                              |
|------------------|-------|--|--|--------|------------------------------|---|--|--------|------------------------------|
|                  |       | $\bar{\theta}$                                       | $\text{stdev}_{\theta}$                              | MSPE   | $\text{stdev}_{\text{MSPE}}$ | $\bar{\theta}$  | $\text{stdev}_{\theta}$                              | MSPE   | $\text{stdev}_{\text{MSPE}}$ |
| $\theta_0^* = 4$ | SS    | $\begin{pmatrix} 4.01 \\ 8.16 \\ 4.75 \end{pmatrix}$ | $\begin{pmatrix} 0.43 \\ 0.78 \\ 0.29 \end{pmatrix}$ | 0.0381 | 0.0209                       | $\begin{pmatrix} 29.03 \\ 7.94 \\ 4.80 \end{pmatrix}$ | $\begin{pmatrix} 1.15 \\ 1.76 \\ 0.11 \end{pmatrix}$ | 0.0332 | 0.0345                       |
|                  | RS    | $\begin{pmatrix} 3.98 \\ 7.97 \\ 4.83 \end{pmatrix}$ | $\begin{pmatrix} 0.06 \\ 0.11 \\ 0.11 \end{pmatrix}$ | 0.0007 | 0.0009                       | $\begin{pmatrix} 29.24 \\ 7.95 \\ 4.79 \end{pmatrix}$ | $\begin{pmatrix} 1.93 \\ 0.26 \\ 0.19 \end{pmatrix}$ | 0.0003 | 0.0003                       |
| $\theta_0^* = 8$ | SS    | $\begin{pmatrix} 4.03 \\ 8.08 \\ 8.77 \end{pmatrix}$ | $\begin{pmatrix} 0.47 \\ 0.86 \\ 0.36 \end{pmatrix}$ | 0.0508 | 0.0522                       | $\begin{pmatrix} 28.39 \\ 7.97 \\ 8.77 \end{pmatrix}$ | $\begin{pmatrix} 1.35 \\ 1.89 \\ 0.13 \end{pmatrix}$ | 0.0528 | 0.0655                       |
|                  | RS    | $\begin{pmatrix} 3.98 \\ 7.98 \\ 8.83 \end{pmatrix}$ | $\begin{pmatrix} 0.07 \\ 0.12 \\ 0.15 \end{pmatrix}$ | 0.0007 | 0.0007                       | $\begin{pmatrix} 28.93 \\ 7.87 \\ 8.78 \end{pmatrix}$ | $\begin{pmatrix} 1.65 \\ 0.31 \\ 0.18 \end{pmatrix}$ | 0.0003 | 0.0003                       |

method, the number of local regions was set to 9 and the number of pseudo inputs was set to 100. In the DDM method, a rectangular mesh was selected with the number of control points on the boundaries and the number of constraining degrees of freedom both set to 3. In the FSA method, the number of knots was set to 50 on a regular grid, the tapering function used was spherical with taper range set to 10. In the training phases for PIC, DDM, and FSA methods, the initial values for each covariance function parameters were randomly selected from the uniform distribution over  $(0, 10]$  in each replicate. The reason for this is that these methods attempt to solve (1.5), which is non-convex, and hence the local minima generated by the optimization solvers highly depend on the initial solution provided. Therefore, to evaluate the performance of these methods in a fair manner, we randomly generate different initial solutions for each replicate. In contrast, our SPS algorithm solves in its first stage a strongly convex problem and hence it does not depend on an initial solution for learning the covariance parameters. The mean and standard deviation of MSPE and parameter estimates for  $N=100$  replications are reported in Table 4.3.

Table 4.3: Comparison of the proposed SPS method against PIC, DDM, and FSA methods for  $N = 100$  simulated data sets of size  $n = 1000$  generated from a GRF with zero mean and SE covariance function ( $\theta^* = (4, 8, 4)^T$ ).

| Method | $\bar{\theta}$                                       | $\text{stdev}_{\theta}$                              | MSPE   | $\text{stdev}_{\text{MSPE}}$ |
|--------|--|--|--------|------------------------------|
| PIC    | $\begin{pmatrix} 5.31 \\ 5.13 \\ 4.74 \end{pmatrix}$ | $\begin{pmatrix} 2.81 \\ 3.01 \\ 2.92 \end{pmatrix}$ | 3.5569 | 1.6096                       |
| DDM    | $\begin{pmatrix} 0.10 \\ 7.95 \\ 4.05 \end{pmatrix}$ | $\begin{pmatrix} 0.15 \\ 1.09 \\ 0.84 \end{pmatrix}$ | 2.6572 | 0.5132                       |
| FSA    | $\begin{pmatrix} 1.99 \\ 0.10 \\ 0.10 \end{pmatrix}$ | $\begin{pmatrix} 2.38 \\ 0.00 \\ 0.00 \end{pmatrix}$ | 6.9692 | 1.0598                       |
| SPS    | $\begin{pmatrix} 4.11 \\ 7.70 \\ 4.97 \end{pmatrix}$ | $\begin{pmatrix} 0.74 \\ 1.21 \\ 0.90 \end{pmatrix}$ | 0.2160 | 0.5060                       |

As it can be seen, the SPS method provides the least biased estimates for all three covariance parameters, with the degree of bias provided by the other methods being much more substantial. Furthermore, the mean

MSPE for the SPS method is considerably lower than that of the other alternatives (one order of magnitude less), and is the least variable. The numerical tests were carried on a desktop computer with Intel Pentium 3.60 GHz CPU and 4 GB memory. The CPU time required by each of the contrasted methods in the learning and prediction stages are displayed in Figure 4.1.

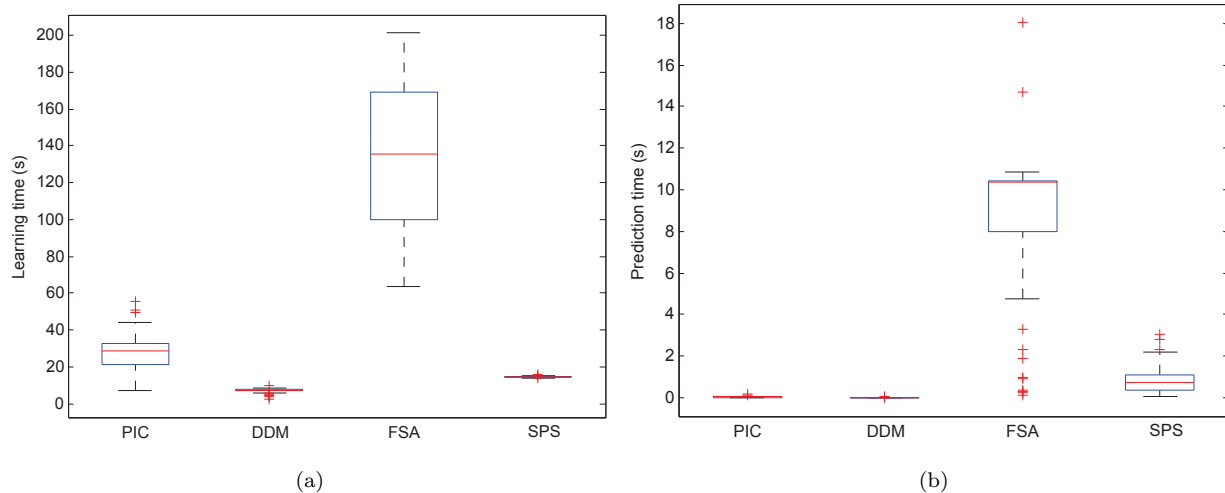


Fig. 4.1: Comparison of learning and prediction times of PIC, DDM, FSA, and SPS methods. **(a)** Learning times **(b)** Prediction times

As we can see from Figure 4.1, for both learning and prediction the DDM method is the fastest and the FSA method the slowest. Of the remaining two methods contrasted, PIC is faster than SPS in the prediction phase but SPS is faster than PIC during learning.

In view of the prediction performance of all the methods compared, the slight speed advantage of DDM over SPS is not a demerit of our method: DDM is unable to provide an unbiased estimate of the range parameter ( $\theta_2^*$ ), crucial in spatial modeling, and this naturally results in considerably worse predictions.

**4.4. Implementation of the SPS method for real data sets.** The first real data set we analyze contains ozone and air quality data as recorded by the Total Ozone Mapping Spectrometer (TOMS) instrument on board the Nimbus-7 satellite. The data set contains 48,331 Total Column Ozone (TCO) measurements over the globe on October 1, 1988 and is available at NASA's website<sup>3</sup>. The second data set we analyzed is the Day/Night Cloud Fraction (CF) from January to September 2009 (size  $n = 64,800$  points) collected by the Moderate Resolution Imaging Spectrometer (MODIS) instrument on board the Terra satellite, a data set also available at NASA's website<sup>4</sup>. A wrapper Matlab function which can read the TCO data with its specific format and produce the input/output matrices is available with our software package at our lab's website<sup>5</sup>. Similarly to the above simulations, 90% of the data was used for learning the covariance parameters and 10% was used for testing. Here, since the true parameters are unknown, we use the response value of 10% randomly selected points as the true response values (cross-validation). The mean and standard deviations of the MSPEs and the parameter estimates for five replicates are reported in Table 4.4 (the test data was randomly selected in each replication). The type of covariance function and blocking scheme were selected based on the best MSPE values obtained.

Since this is real data, we cannot make any judgment about the parameter estimates; however, the standard deviations are quite small relative to the parameter estimate magnitudes for both data sets. Furthermore, comparing MSPEs with the data magnitudes confirms good model fits to the data sets.

<sup>3</sup><http://ozoneaq.gsfc.nasa.gov/nimbus7Ozone.md>

<sup>4</sup>[http://gdata1.sci.gsfc.nasa.gov/daac-bin/G3/gui.cgi?instance\\_id=MODIS\\_MONTHLY\\_L3](http://gdata1.sci.gsfc.nasa.gov/daac-bin/G3/gui.cgi?instance_id=MODIS_MONTHLY_L3)

<sup>5</sup><http://www2.ie.psu.edu/Castillo/research/engineeringstatistics/software.htm>

Table 4.4: Implementation of the proposed SPS method for two real data sets, TCO and CF, with performance measures computed over 5 replicated cross-validations (10% of data randomly sampled for testing, 90% for learning).

| Data | Covariance Function | Block | $\bar{\theta}$  | $\text{stdev}_{\theta}$                              | $\overline{\text{MSPE}}$ | $\text{stdev}_{\text{MSPE}}$ |
|------|---------------------|-------|---|--|--------------------------|------------------------------|
| TCO  | Matern              | RS    | $\begin{pmatrix} 12.20 \\ 1098 \\ 0.00 \end{pmatrix}$ | $\begin{pmatrix} 0.01 \\ 0.54 \\ 0.00 \end{pmatrix}$ | 4.5361                   | 0.0623                       |
| CF   | Exponential         | RS    | $\begin{pmatrix} 10.07 \\ 0.05 \\ 0.82 \end{pmatrix}$ | $\begin{pmatrix} 0.04 \\ 0.00 \\ 0.00 \end{pmatrix}$ | 0.0044                   | 0.0000                       |

**5. Conclusions and further research.** A new GRF estimation method was presented and compared to alternative methods. The new distance-based Sparse Precision matrix Selection (SPS) method provides considerably better parameter estimates and hence considerable better predictions compared to other recently proposed methods for large-scale GRF estimation. The proposed algorithm can be used to fit a GRF to large data sets using a blocking scheme which allows for parallelization of the method. The learning phase consists of two stages: in the first stage, a sparse precision matrix is directly estimated from the data through the optimization of a convex regularized ML objective using the Alternating Directions Method of Multipliers (ADMM) algorithm, which converges linearly for our GRF model fitting problem. The output of this stage implies a GMRF approximation to the GRF, but unlike similar approximations, we let the data determine the sparsity pattern and use the inter-point distances as weights in the regularization term. In the second stage, the covariance parameter estimates are obtained by minimizing the Frobenius distance between the parametric covariance matrix corresponding to the observed locations  $\mathcal{D}^x$  and the inverse of the sparse precision matrix obtained in stage one. Two blocking schemes, Spatial Segmentation (SS) and Random Selection (RS), were proposed for partitioning large data sets. Numerical results in Section 4 demonstrate the capability of the SPS method for efficiently estimating the covariance function parameters, which in turn results in mean squared prediction errors one order of magnitude less than those obtained with competing methods. In the case of a stationary GRF, the proposed approach provides a predicted surface that has no discontinuities along the boundary points between blocks since only a single covariance matrix over the full domain is estimated in the second stage.

The following are some further lines of investigation we plan to pursue in the near future.

It was shown numerically that as the number of locations  $n$  grows in a bounded domain  $\mathcal{X} \subset \mathbb{R}^d$ , the precision matrices of a stationary, isotropic GRF become near-sparse at a faster rate in  $n$  than the corresponding covariance matrices. Future work should provide a theoretical analysis of this observed behavior of the precision matrix under infill asymptotics ( $n \rightarrow \infty$ ) for a given covariance function.

Another problem of interest is to try to find error bounds on  $\|\hat{P} - P^*\|_F$  as a function of the number of GRF realizations  $N_r$ , where  $\hat{P}$  is the estimated precision matrix in our Stage 1 and  $P^* = C(\theta^*)^{-1} \in \mathbb{R}^{n \times n}$  is the true precision matrix of the GRF over a fixed set of  $n$  locations in  $\mathcal{X}$ . In the present paper we assumed  $N_r = 1$ , but the performance of our method under repeated sampling should be investigated as well.

**Appendix A.** Here, we show how the optimization problem (3.23) for *isotropic* covariance functions with nugget can be simplified to a one-dimensional line search in the range parameter. Isotropic covariance functions correspond to isotropic GRFs in which the covariance between any two points is a function of their distance but not of the direction of the vector connecting the two [40]. Furthermore, an isotropic covariance function can be written as  $c(\theta, \mathbf{x}, \mathbf{x}') = \theta_1 r(\|\mathbf{x} - \mathbf{x}'\|, \theta_2) + \theta_0 \delta(\mathbf{x}, \mathbf{x}')$  where  $r(\cdot, \theta_2)$  is an isotropic correlation function,  $\theta_0$ ,  $\theta_1$ ,  $\theta_2$  are the nugget, variance, range parameters, respectively, and  $\delta(\cdot, \cdot)$  is the indicator function such that  $\delta(\mathbf{x}, \mathbf{x}') = 1$  if  $\mathbf{x} = \mathbf{x}'$ , and equal to 0 otherwise. Equations (A.1), (A.2), (A.3) show the Exponential, Square-Exponential (SE), and Matern ( $\nu = 3/2$ ) correlation functions that were referred to in



the main part of this paper, namely:

$$r(\|\mathbf{x} - \mathbf{x}'\|, \theta_2) = \exp\left(\frac{-\|\mathbf{x} - \mathbf{x}'\|}{\theta_2}\right), \quad (\text{A.1})$$

$$r(\|\mathbf{x} - \mathbf{x}'\|, \theta_2) = \exp\left(\frac{-\|\mathbf{x} - \mathbf{x}'\|^2}{\theta_2^2}\right), \quad (\text{A.2})$$

$$r(\|\mathbf{x} - \mathbf{x}'\|, \theta_2) = \left(1 + \frac{\sqrt{3}\|\mathbf{x} - \mathbf{x}'\|}{\theta_2}\right) \exp\left(\frac{-\sqrt{3}\|\mathbf{x} - \mathbf{x}'\|}{\theta_2}\right). \quad (\text{A.3})$$

Let  $D_k \in \mathbb{R}^{n_k \times n_k}$  denote the Euclidean pairwise distance matrix corresponding to block  $k$ : for all  $(i, j) \in \mathcal{I}_k \times \mathcal{I}_k$ ,  $(D_k)_{ij} = \|\mathbf{x}_i - \mathbf{x}_j\|_2$ . Note that as opposed to  $G_k$  defined in (3.2),  $(D_k)_{ii} = 0$  for all  $i \in \mathcal{I}_k$ . Then, (3.23) can be written as

$$\min_{\theta_0 \geq 0, \theta_1 \geq 0, \theta_2 \geq 0} \sum_{k=1}^K \sum_{i,j \in \mathcal{I}_k} \left( (C_k)_{ij} - \theta_1 r((D_k)_{ij}, \theta_2) - \theta_0 \delta(i, j) \right)^2, \quad (\text{A.4})$$

where  $(C_k)_{ij}$  is the  $(i, j)$ -th element of  $\hat{P}_k^{-1}$ , and  $\delta(i, j) = 1$  if  $i = j$ , and equal to 0 otherwise. The optimization problem (A.4) can be written sequentially as

$$\underset{\theta_2 \geq 0}{\text{minimize}} \left( \underset{\theta_0 \geq 0, \theta_1 \geq 0}{\text{minimize}} \sum_{k=1}^K \sum_{i,j \in \mathcal{I}_k} \left( (C_k)_{ij} - \theta_1 r((D_k)_{ij}, \theta_2) - \theta_0 \delta(i, j) \right)^2 \right). \quad (\text{A.5})$$

The inner optimization problem can be written as

$$\underset{\theta_0 \geq 0, \theta_1 \geq 0}{\text{minimize}} \quad \|\mathbf{c} + \theta_1 \mathbf{r}(\theta_2) + \theta_0 \mathbf{d}\|_2^2, \quad (\text{A.6})$$

where  $\|\cdot\|_2$  is the vector 2-norm and  $\mathbf{c}$ ,  $\mathbf{r}$ , and  $\mathbf{d}$  are *long vectors* in  $\mathbb{R}^{\sum_{k=1}^K n_k^2}$  such that  $\mathbf{c}_{ij} = (C_k)_{ij}$ ,  $(\mathbf{r}(\theta_2))_{ij} = -r((D_k)_{ij}, \theta_2)$ , and  $\mathbf{d}_{ij} = -\delta(i, j)$  for  $(i, j) \in \mathcal{I}_k$  and  $k = 1, \dots, K$ . The Lagrangian for the problem (A.6) is

$$L(\theta_0, \theta_1; \beta_2, \beta_3) = \|\mathbf{c} + \theta_1 \mathbf{r}(\theta_2) + \theta_0 \mathbf{d}\|_2^2 - \beta_2 \theta_1 - \beta_3 \theta_0.$$

Using the first order optimality condition and solving for the two Lagrange multipliers, we get

$$\beta_2 = 2\mathbf{r}(\theta_2)^T (\mathbf{c} + \theta_1 \mathbf{r}(\theta_2) + \theta_0 \mathbf{d}), \quad (\text{A.7a})$$

$$\beta_3 = 2\mathbf{d}^T (\mathbf{c} + \theta_1 \mathbf{r}(\theta_2) + \theta_0 \mathbf{d}). \quad (\text{A.7b})$$

Replacing  $\beta_2$  and  $\beta_3$  in the Complementary Slackness conditions,  $\beta_2 \theta_1 = 0$  and  $\beta_3 \theta_0 = 0$ , and solving for  $\theta_0$  and  $\theta_1$ , we get four solutions:

1.  $(\theta_1 = 0, \theta_0 = \frac{-\mathbf{d}^T \mathbf{c}}{\|\mathbf{d}\|_2^2})$
2.  $(\theta_1 = \frac{-\mathbf{r}(\theta_2)^T \mathbf{c}}{\|\mathbf{r}(\theta_2)\|_2^2}, \theta_0 = 0)$
3.  $(\theta_1 = \frac{(\mathbf{r}(\theta_2)^T \mathbf{d})(\mathbf{d}^T \mathbf{c}) - (\mathbf{r}(\theta_2)^T \mathbf{c})\|\mathbf{d}\|_2^2}{\|\mathbf{r}(\theta_2)\|_2^2 \|\mathbf{d}\|_2^2 - (\mathbf{r}(\theta_2)^T \mathbf{d})^2}, \theta_0 = \frac{(\mathbf{r}(\theta_2)^T \mathbf{d})(\mathbf{r}(\theta_2)^T \mathbf{c}) - (\mathbf{d}^T \mathbf{c})\|\mathbf{r}(\theta_2)\|_2^2}{\|\mathbf{r}(\theta_2)\|_2^2 \|\mathbf{d}\|_2^2 - (\mathbf{r}(\theta_2)^T \mathbf{d})^2})$
4.  $(\theta_1 = 0, \theta_0 = 0)$

Hence, for any fixed value of  $\theta_2$  in the outer optimization problem in (A.5), which is solved by Bisection, we need to evaluate all of the four solutions above; the solution where both  $\theta_0$  and  $\theta_1$  are nonnegative and results in the minimum function value is the optimal solution to the inner problem. In this way, the optimization (A.4) is simplified to a one-dimensional line search in the space of the range parameter  $\theta_2$ .

## REFERENCES

- [1] N. S. AYBAT AND G. IYENGAR, *An alternating direction method with increasing penalty for stable principal component pursuit*. arXiv:1309.6553 [math.OC], 2014.
- [2] SUDIPTO BANERJEE, ALAN E. GELFAND, ANDREW O. FINELY, AND HUIYAN SANG, *Gaussian predictive process models for large spatial data sets*, Journal of Royal Statistical Society, 70 (2008), pp. 825–848.
- [3] JULIAN BESAG, *Spatial Interaction and the Statistical Analysis of Lattice Systems*, Journal of the Royal Statistical Society. Series B (Methodological), 36 (1974), pp. 192–236.
- [4] CHRISTOPHER M. BISHOP, *Pattern Recognition and Machine Learning*, Information Science and Statistics, Springer, 2009.
- [5] G.E.P. BOX, G.M. JENKINS, AND G.C. REINSEL, *Time Series Analysis: Forecasting and Control*, Wiley Series in Probability and Statistics, Wiley, 2008.
- [6] STEPHEN BOYD, NEAL PARIKH, ERIC CHU, BORJA PELEATO, AND JONATHAN ECKSTEIN, *Distributed optimization and statistical learning via the alternating direction method of multipliers*, Foundations and Trends® in Machine Learning, 3 (2011), pp. 1–122.
- [7] NOEL CRESSIE AND GARDAR JOHANNESSON, *Fixed rank kriging for very large spatial data sets*, Journal of Royal Statistical Society, 70 (2008), pp. 209–226.
- [8] NOEL A. C. CRESSIE, *Statistics for spatial data*, John Wiley and Sons, 1993.
- [9] A. D’ASPROMONT, O. BANERJEE, AND GHAOU L. EL., *First-order methods for sparse covariance selection*, SIAM Journal on Matrix Analysis and Applications, 30 (2008), pp. 56–66.
- [10] A. P. DEMPSTER, *Covariance selection*, Biometrics, 28 (1972), pp. pp. 157–175.
- [11] W. DENG AND W. YIN, *On the global and linear convergence of the generalized alternating direction method of multipliers*. Rice CAAM technical report 12-14, 2012.
- [12] J. ECKSTEIN, *Augmented lagrangian and alternating direction methods for convex optimization: A tutorial and some illustrative computational results*, Tech. Report Rutcor Research Report RRR 32-2012, Rutgers Center for Operations Research, December 2012.
- [13] J. ECKSTEIN AND D. P. BERTSEKAS, *On the douglas-rachford splitting method and the proximal point algorithm for maximal monotone operators*, Mathematical Programming, 55 (1992), pp. 293–318.
- [14] JEROME FRIEDMAN, TREVOR HASTIE, AND ROBERT TIBSHIRANI, *Sparse inverse covariance estimation with the graphical lasso*, Biostatistics, 9 (2008), pp. 432–441.
- [15] MONTSERRAT FUENTES, *Approximate likelihood for large irregularly spaced spatial data*, Journal of American Statistical Association, 102 (2007), pp. 321–331.
- [16] M. FUKUSHIMA, *Application of the alternating direction method of multipliers to separable convex programming problems*, Computational Optimization and Applications, 1 (1992), p. 93111.
- [17] REINHARD FURRER, MARC G. GENTON, AND DOUGLAS W. NYCHKA, *Covariance tapering for interpolation of large spatial datasets*, Journal of Computational and Graphical Statistics, 15 (2006), pp. 502–523.
- [18] R. GLOWINSKI, *Augmented Lagrangian Methods: Applications to the Numerical Solution of Boundary-Value Problems*, Studies in Mathematics and its Applications, Elsevier Science, 2000.
- [19] ROBERT B GRAMACY AND DANIEL W APLEY, *Local gaussian process approximation for large computer experiments*, arXiv preprint arXiv:1303.0383, (2013).
- [20] B. HE AND H. YANG, *Some convergence properties of a method of multipliers for linearly constrained monotone variational inequalities*, Operations Research Letters, 23 (1998), pp. 151–161.
- [21] B. HE, H. YANG, AND S.L. WANG, *Alternating direction method with self-adaptive penalty parameters for monotone variational inequalities*, Journal of Optimization Theory and Applications, 106 (2000), pp. 337–356.
- [22] DAVE HIGDON, *Space and space-time modeling using process convolutions*, in Quantitative Methods for Current Environmental Issues, CliveW. Anderson, Vic Barnett, PhilipC. Chatwin, and AbdelH. El-Shaarawi, eds., Springer London, 2002, pp. 37–56.
- [23] JEAN HONORIO AND TOMMI S. JAAKKOLA, *Inverse covariance estimation for high-dimensional data in linear time and space: Spectral methods for riccati and sparse models*, Tech. Report arXiv:1309.6838, 2013.
- [24] A. G. JOURNAL AND CH. J. HUIJBREGTS, *Minning Geostatistics*, Academic Press, 1978.
- [25] S. KONTOGIORGIS AND R. R. MEYER, *A variable-penalty alternating direction method for convex optimization*, Mathematical Programming, 83 (1998), pp. 29–53.
- [26] A.S. LEWIS, *The convex analysis of unitarily invariant matrix functions*, Journal of Convex Analysis, 2 (1995), pp. 173–183.
- [27] FAMING LIANG, YICHEN CHENG, QIFAN SONG, JINCHEOL PARK, AND PING YANG, *A resampling-based stochastic approximation method for analysis of large geostatistical data*, Journal of the American Statistical Association, 108 (2013), pp. 325–339.
- [28] FINN LINDGREN, HVAR D RUE, AND JOHAN LINDSTRM, *An explicit link between gaussian fields and gaussian markov random fields: the stochastic partial differential equation approach*, Journal of the Royal Statistical Society: Series B (Statistical Methodology), 73 (2011), pp. 423–498.
- [29] P. L. LIONS AND B. MERCIER, *Splitting algorithms for the sum of two nonlinear operators*, SIAM Journal on Numerical Analysis, 16 (1979), p. 964979.
- [30] K. V. MARDIA AND A. J. WATKINS, *On multimodality of the likelihood in the spatial linear model*, Biometrika, 76 (1989), pp. 289–295.
- [31] RAHUL MAZUMDER AND TREVOR HASTIE, *Exact covariance thresholding into connected components for large-scale graphical lasso*, Journal of Machine Learning Research, 13 (2012), pp. 781–794.
- [32] KEVIN P. MURPHY, *Machine Learning: A Probabilistic Perspective*, MIT Press, 2012.
- [33] DOUGLAS NYCHKA, SOUTIR BANDYOPADHYAY, DORIT HAMMERLING, FINN LINDGREN, AND STEPHAN SAIN, *A multi-resolution gaussian process model for the analysis of large spatial data sets*, tech. report, 2012.

- [34] CHIWOO PARK, JIANHUA Z. HUANG, AND YU DING, *Domain decomposition approach for fast gaussian process regression of large spatial data sets*, J. Mach. Learn. Res., 12 (2011), pp. 1697–1728.
- [35] HAVARD RUE AND LEONHARD HELD, *Gaussian Markov Random Fields: Theory and Applications*, Chapman & Hall/CRC, 2005.
- [36] HAVARD RUE AND HAKON TJELMELAND, *Fitting gaussian markov random fields to gaussian fields*, Scandinavian Journal of Statistics, 29 (2002), pp. 31–49.
- [37] HUIYAN SANG AND JIANHUA Z. HUANG, *A full scale approximation of covariance functions for large spatial data sets*, Journal of Royal Statistical Society, 71 (2012), pp. 111–132.
- [38] DANIEL SIMPSON, FINN LINDGREN, AND HVARD RUE, *Think continuous: Markovian gaussian models in spatial statistics*, Spatial Statistics, 1 (2012), pp. 16 – 29.
- [39] EDWARD SNELSON AND ZOUBIN GHAHRAMANI, *Local and global sparse gaussian process approximations*, in International Conference on Artificial Intelligence and Statistics, 2007, pp. 524–531.
- [40] MICHAEL L. STEIN, *Interpolation of Spatial Data: Some Theory for Kriging*, Springer Series in Statistics, Springer, 1999.
- [41] MICHAEL L. STEIN, ZHIYI CHI, AND LEAH J. WELTY, *Approximating likelihoods for large spatial data sets*, journal of Royal Statistical Society, 66 (2004), pp. 275–296.
- [42] A. V. VECCHIA, *Estimation and model identification for continuous spatial processes*, journal of Royal Statistical Society, 50 (1988), pp. 297–312.
- [43] J. J. WARNES AND B. D. RIPLEY, *Problems with likelihood estimation of covariance functions of spatial gaussian processes*, Biometrika, 74 (1987), pp. 640–642.
- [44] JOE WHITTAKER, *Graphical Models in Applied Multivariate Statistics*, John Wiley, 2009.
- [45] XIAOMING YUAN, *Alternating direction method for covariance selection models*, Journal of Scientific Computing, 51 (2012), pp. 261–273.